NJC

Accepted Manuscript

This is an *Accepted Manuscript*, which has been through the Royal Society of Chemistry peer review process and has been accepted for publication.

Accepted Manuscripts are published online shortly after acceptance, before technical editing, formatting and proof reading. Using this free service, authors can make their results available to the community, in citable form, before we publish the edited article. We will replace this *Accepted Manuscript* with the edited and formatted *Advance Article* as soon as it is available.

You can find more information about *Accepted Manuscripts* in the Information for Authors.

Please note that technical editing may introduce minor changes to the text and/or graphics, which may alter content. The journal's standard Terms & Conditions and the Ethical guidelines still apply. In no event shall the Royal Society of Chemistry be held responsible for any errors or omissions in this *Accepted Manuscript* or any consequences arising from the use of any information it contains.

ROYAL SOCIETY OF CHEMISTRY

www.rsc.org/njc

Novel synergistic photocatalytic degradation of antibiotics and bacteria using V-N doped TiO_2 under visible light: State of nitrogen in V-doped TiO_2

*Neerugatti KrishnaRao Eswar [1], Praveen C Ramamurthy [1,2] and Giridhar Madras [3]**

[1]Centre for Nanoscience and Engineering, [2]Dept. of Materials Engineering,

[3]Dept. of Chemical Engineering, Indian Institute of Science, Bangalore-560012

Abstract

We report the synthesis of vanadium and nitrogen co-doped TiO_2 for photocatalysis mainly emphasizing on the state of nitrogen doping into TiO_2 in the presence of vanadium ions. Considering the increase in antibiotic resistance developed by microbes due to excess of pharmaceutical wastes in the ecosystem, the photocatalytic activity was measured by degrading an antibiotic, chloramphenicol. A novel experiment was conducted by degrading the antibiotic and bacteria in their close vicinity to focus on their synergistic photo-degradation by V-N co-doped TiO_2. The catalysts were characterized using XRD, DRS, PL, TEM, BET and XPS analysis. Both interstitial and substitutional nitrogen doping was achieved with the V-TiO_2, showing high efficiency under visible light for antibiotic and bacteria degradation. In addition, the effect of doping concentration of nitrogen and vanadium in TiO_2 and catalyst loading was studied thoroughly. Reusability experiments show that the prepared V-N co-doped TiO_2 was stable for many cycles.

Keywords: *V-N TiO_2; interstitial and substitutional nitrogen; photocatalysis; antibiotic; bacteria, degradation.*

* Corresponding author. Tel. +91 80 22932321; Fax: +91 80 23600683,
E-mail: giridhar@chemeng.iisc.ernet.in (G. Madras)

1. Introduction

Photocatalysis is one of the highly effective advanced oxidation processes for waste water treatment. Semiconductors are employed as photocatalysts for water purification for the degradation of organics [1]. Among all semiconductors, TiO_2 is extensively used because of its non-toxicity, stability and availability[2]; however, it is active only under UV illumination. Therefore, significant research has been conducted to extend the light absorption of TiO_2 towards visible region [3, 4]. This is achieved by doping metals and non-metals [5-12] and also by preparing nanocomposites of TiO_2 with visible light absorbing semiconductors [13-16] etc. Basically, transition metal ions such as V, Mn, Cu, Fe, Cr [17-20] and non-metals like N, S, B, and C [21-25] are doped into TiO_2 for the prevention of recombination, efficient charge separation, and reducing the band gap. However, an increase in concentration of these dopants decreases the photocatalytic activity by promoting recombination.

Among non-metals, research has been conducted on doping nitrogen in TiO_2 and it has been studied for its structural and optical properties [26, 27]. N doped TiO_2 yielded significant improvement in visible light photocatalytic activity[28-31]. However, the doping of N can be either in substitutional or interstitial sites but it is not clear which doping is more favorable[32, 33]. In addition, metal - non-metal and bimetallic co-doping such as N and various metals [34], N and Ce [35], Zn and Fe [36], Cu and I [37], V and N [38-40] , Bi and B[41], Bi and N[42], Ce and N[43], Fe and N[44, 45], Fe and S[46], La and N[47], V and C[48], Yb and N[49] into TiO_2 has proven to enhance the visible light photocatalytic activity. Among the transition metal ions dopants for TiO_2, the presence of variable oxidation states (V^{3+}, V^{4+}, V^{5+}) and comparable ionic size (V_r^{ion} ~ 68 - 78 pm) with respect to Ti (Ti_r^{ion} ~ 75 pm) favors vanadium as an effective dopant. The presence of low concentration of vanadium in TiO_2 lattice efficiently prevents the electron – hole recombination by having V^{4+} and V^{5+} interactions and also increases visible light absorption [39, 40]. Only few reports are available on the photocatalytic activity of V-TiO_2 and V-N

TiO_2 such as for its use in oxidation of ethanol [50], degradation of methyl blue dye [38], pentachlorophenol [39] and Rhodamine B [40] under visible light illumination.

Photocatalysis is not only employed for the degradation of chemical contaminants but also for the inactivation of microorganisms. The reactive oxygen radicals produced during photocatalysis kill the bacteria by co-enzyme oxidation, nucleic acid attack, peroxidation of lipids and by dis-organizing cell membrane[51-54]. Antibiotics play a major role in reducing the mortality rate of organisms by combating infectious diseases [55]. Understanding the mechanism of infections and the response of pathogens with respect to hosts helps in formulating the synthetic antibiotics. These antibiotics can inactivate the microbes by inhibiting the cell wall, protein, DNA, RNA, folic acid synthesis and also disorganize bacterial membranes [56]. Since production of synthetic antibiotics has become fully industrialized, the possibility of antibiotic pollution in effluents has significantly risen recently [57, 58]. These antibiotic pollutants persist for a long time since they are not easily degradable and have long time biological responses. In this specific type of pollution, the pollutant becomes a favorable agent for microbes in developing a resistance towards the antibiotics, which are lately referred as "super bugs" [59, 60].

This resistance developed by the microorganism is a serious concern as it poses a major threat not only to the environment but also prevents treatment opportunities for an infected host. Microbes that show resistance towards many antibiotics are termed as "multidrug resistant" [61]. These resistances increase rapidly due to exposure of antibiotics from various sources such as improperly treated pharmaceutical effluent streams [62].

Therefore, in this current study, we have prepared vanadium, nitrogen co-doped TiO_2 catalysts for the synergistic degradation of antibiotics and microbes both separately and also in their close

vicinity. The catalysts were characterized using XRD, DRS, TEM and XPS studies. The novelty of this study is two-fold. This is the first work to emphasize the inactivation of microbes in the presence of antibiotics showing both degradation of microbes and also antibiotics simultaneously. This is also the first work that emphasizes the state of nitrogen doping in vanadium doped TiO_2 and its influence on the mechanism and activity for the photocatalytic inactivation of microorganisms.

2. Experimental

2.1. Materials

Titanium butoxide (>97% purity, Sigma-Aldrich, USA). LB broth, nutrient agar and chloramphenicol ($C_{11}H_{12}Cl_2N_2O_5$, potency ~900 µg/mg) were procured from Hi-Media (India) Pvt. Ltd. Ammonium meta-vanadate (99% pure, SD Fine chemicals, India, Ltd). Triethylamine (>99% pure) and nitric acid were obtained from Merck (India) Ltd. All the experiments were done using Millipore water.

2.2. Catalyst preparation

2.2.1. Synthesis of vanadium doped TiO_2

Vanadium doped TiO_2 was synthesized using sol-gel precipitation. Initially, stoichiometric amount of ammonium vanadate was dissolved in 500 ml of deionized water and stirred for 1 h. Similarly, a stoichiometric amount of titanium butoxide was dissolved in iso-propyl alcohol and this solution was added drop wise into an aqueous solution containing vanadium ions. The pH of 2 was then obtained using nitric acid (1 M). This mixture was stirred continuously for 24 h and then evaporated at 50º C. Later, all the samples were calcined at 400ºC in a muffle furnace. Various V-doped TiO_2 samples were prepared by maintaining the vanadium concentration as 0.1, 0.2, 1 and 2 atom % with respect

to Ti [39]. Pristine TiO_2 without vanadium doping was also prepared according to the same procedure, as mentioned above except for the addition of ammonium vanadate.

2.2.2. Synthesis of nitrogen vanadium co-doped TiO_2

Nitrogen vanadium co-doped TiO_2 samples were synthesized using hydrothermal method. Initially excess than stoichiometric amount of triethylamine was taken in deionized water and stirred continuously for 1 h. 0.1 g of vanadium doped TiO_2 samples were dispersed in the above solution using ultrasonication. The finely dispersed solution was placed in a Teflon beaker covered with stainless steel autoclave and kept at 180ºC for 20 h [38]. Various N-doped V-TiO_2 samples were prepared by maintaining the concentration of nitrogen as 0.5, 1, 2, 4 atom % with respect to Ti. The products were allowed to cool to 25 ºC and then washed with deionized water twice and ethanol thrice. Later, the washed samples were kept for drying at 70ºC for 10 h. Pristine nitrogen doped samples (0.5, 1, 2 and 4 atom %) were prepared by using hydrothermal reaction of pristine TiO_2 in triethylamine solution.

2.3. Catalyst characterization

Rigaku diffractometer with Cu-Kα radiation was used to capture XRD patterns. ULTRA55 FESEM, Carl Zeiss was used to obtain SEM images. Samples dispersed in absolute ethanol were drop-casted on Si wafers and kept under vacuum for 12 h; Samples were gold sputtered using Quorum sputtering. TEM pictures were acquired by FEI Tecnai T-20 at 180 kV. TEM samples were prepared drop casting iso-propanol dispersed particles on Cu grids and kept under vacuum for 24 h. Perkin Elmer, Lambda 35, UV-visible spectrophotometer was used to measure DRS. Shimadzu-UV 1700, UV-visible spectrophotometer was used to determine absorbance of photocatalysis samples. Photoluminescence spectra were taken using PL-Spectrophotometer (Perkin Elmer) with excitation

wavelength at 365 nm. Catalyst particles were regenerated at 120 °C for 2 h prior and Nova-1000 Quantachrome was used for BET surface analysis. X-ray photoelectron spectroscopic data was obtained using AXIS ULTRA.

2.4. Photocatalysis

2.4.1. Photochemical reactor

The photocatalysis experiments were performed using 25 ppm aqueous solution of chloramphenicol under 400 W metal halide lamp (Philips - India) having λ_{max}, intensity and photon flux of 510 nm, of the order 10^{-7} and 220 μW cm^{-2}, respectively. A $K_2Cr_2O_7$ UV solution cut-off filter was used to restrict the UV light emitted from the metal halide lamp. 1 g/l catalyst concentration was kept for all the experiments unless stated otherwise. Catalyst was taken in the antibiotic solution for 60 min to observe adsorption-desorption equilibrium. The samples after the photochemical reactions were collected at regular time intervals, centrifuged and measured for absorbance using UV-visible spectrophotometer.

2.4.2. Antibacterial evaluation

All the plating accessories, broth and agar media were autoclaved before conducting the experiments. *Escherichia coli* (K-12, MG1655, Gram negative) were cultured using liquid nutrient broth. Bacterial pellet was collected by centrifuging the culture medium at 5000 rpm for 10 min. Bacterial suspension was obtained by suspending the pellet in sterile water. Sterilized nutrient agar was decanted into petri plates for solidification. Dark experiments without light irradiation were carried out with 1 g/l catalyst in the bacterial suspension. Later, bacterial solution with catalyst particles was irradiated by visible light. Samples were collected at specific intervals to quantify the

antibacterial activity. 100 µl serial diluted samples was spread onto nutrient agar plates and incubated at 37°C for 24 h. The experiment was further iterated and the bacterial colonies were quantified.

2.4.3. Simultaneous degradation of antibiotics and inactivation of bacteria

For degradation of antibiotics and inactivation of bacteria, the centrifuged bacterial pellet obtained from the culture was suspended in deionized water containing 25 ppm of antibiotic (Chloramphenicol, λ_{max} – 278 nm). Prior to that, the bacterial culture was tested for its resistance against the antibiotic using spread plate technique. Later catalyst particles were added to the above solution and stirred continuously under visible light. Periodically, the samples were collected for nutrient agar plating and also for antibiotic absorbance measurements. The spreaded nutrient agar plate was then incubated at 37ºC for 24 h. All the experiments mentioned in the sections 2.4.1, 2.4.2 and 2.4.3 in triplicate were conducted.

3. Results and Discussion

V doped TiO_2 was successfully synthesized using simple sol-gel route. N doped TiO_2 and nitrogen in V-N co-doped TiO_2 was synthesized using hydrothermal technique. The quantity of vanadium was varied as 0.1, 0.2, 1 and 2 atom % and they were named as V0.1, V0.2, V1 and V2 respectively. Similarly, quantity of N was varied as 0.5, 1, 2 and 4 atom % and named as N0.5, N1, N2 and N4 respectively. The vanadium concentration was maintained as 2 atom % (best photoactivity as in V-TiO_2) in V-N co-doped TiO_2 whereas the concentration of nitrogen was varied as 1 and 2 atom % and named as V2N1 and V2N2, respectively. All the characterization studies were done for best compositions viz. N2-TiO_2, V2-TiO_2, V2N1-TiO_2 and V2N2-TiO_2, unless mentioned otherwise.

3.1. Characterization studies

In order to identify the crystal structure of the synthesized catalysts, X-ray diffraction patterns of undoped TiO_2 and all compositions of V-N TiO_2 are shown in the Fig. 1. The presence of nitrogen in the TiO_2 lattice favors formation of anatase, because of large ionic radius of N^{3-} compared to O^{2-}. Similarly doping with vanadium in V^{4+}/V^{5+} state, whose ionic radius is less than Ti, facilitates charge neutrality and also allows substitution of O^{2-} with N^{3-} in the TiO_2 lattice without distorting TiO_2 structure [63]. No peaks corresponding to oxides of vanadium were observed. Similarly, no phase separation of TiO_2 was observed. Therefore, it can be inferred that vanadium ion has been completely substituted into the crystal lattice of the titania. (101), (004), (200), (211) and (204) are the planes found in all the catalysts which shows no presence of rutile phase in all catalysts. The width of the (101) peak shows a broadening while intensity increases with an increase in the nitrogen and vanadium concentration. In addition, a small shift occurs due to the replacement of high density oxygen atom by low density nitrogen atom in the TiO_2 lattice due to nitrogen incorporation during doping [64]. This indicates that a stress is created due to the difference in the bonding characteristics between nitrogen and oxygen. This replacement leads to a change in electronic states and optical absorption.

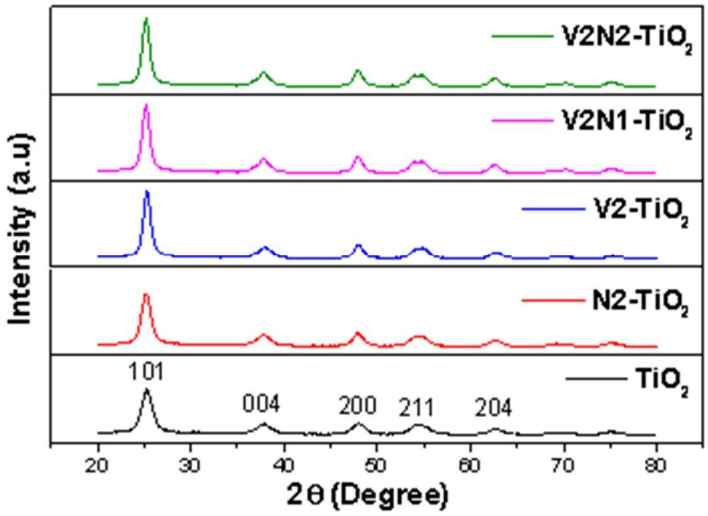

Fig. 1. X-ray diffraction pattern of V2-TiO_2, N2-TiO_2, V2N1-TiO_2, V2N2-TiO_2 co-doped catalyst

Catalyst	Crystallite Size (nm)	Surface area (m^2/g)
TiO_2	7.69	196
N2-TiO_2	8.92	178
V2-TiO_2	11.59	184
V2N1-TiO_2	11.30	163
V2N2-TiO_2	11.34	156

Table 1: Crystallite size and surface area of TiO_2, N2- TiO_2, V2- TiO_2, V2N1- TiO_2 and V2N2- TiO_2

Table 1 shows the crystallite size calculated from XRD and the surface areas of the catalysts. The BET surface areas of TiO_2, N2-TiO_2, V2-TiO_2, V2N1-TiO_2 and V2N2-TiO_2 were found to be 196, 178, 188, 163 and 156 m^2/g, respectively. In addition to that, the crystallite size of pristine TiO_2 is lesser compared to all other doped samples, which can be observed from XRD (Fig.1). The

crystallite size of N2-TiO_2 is larger than TiO_2, because of nitridation process where nanocrystals tend to aggregate. However, cationic (V) doping into TiO_2 has not increased the crystallite size but changed the surface area. Co-doping of V and N into TiO_2 has decreased the surface area significantly. The transmission electron microscopic images of V2N1-TiO_2 and undoped TiO_2 are shown in Fig. 2 (a), (b) and (c), (d) respectively. The catalyst particles were spherical in shape and around 10 nm in size. There are no fringes observed for vanadium oxide indicating vanadium exists in dopant form into the TiO_2 lattice.

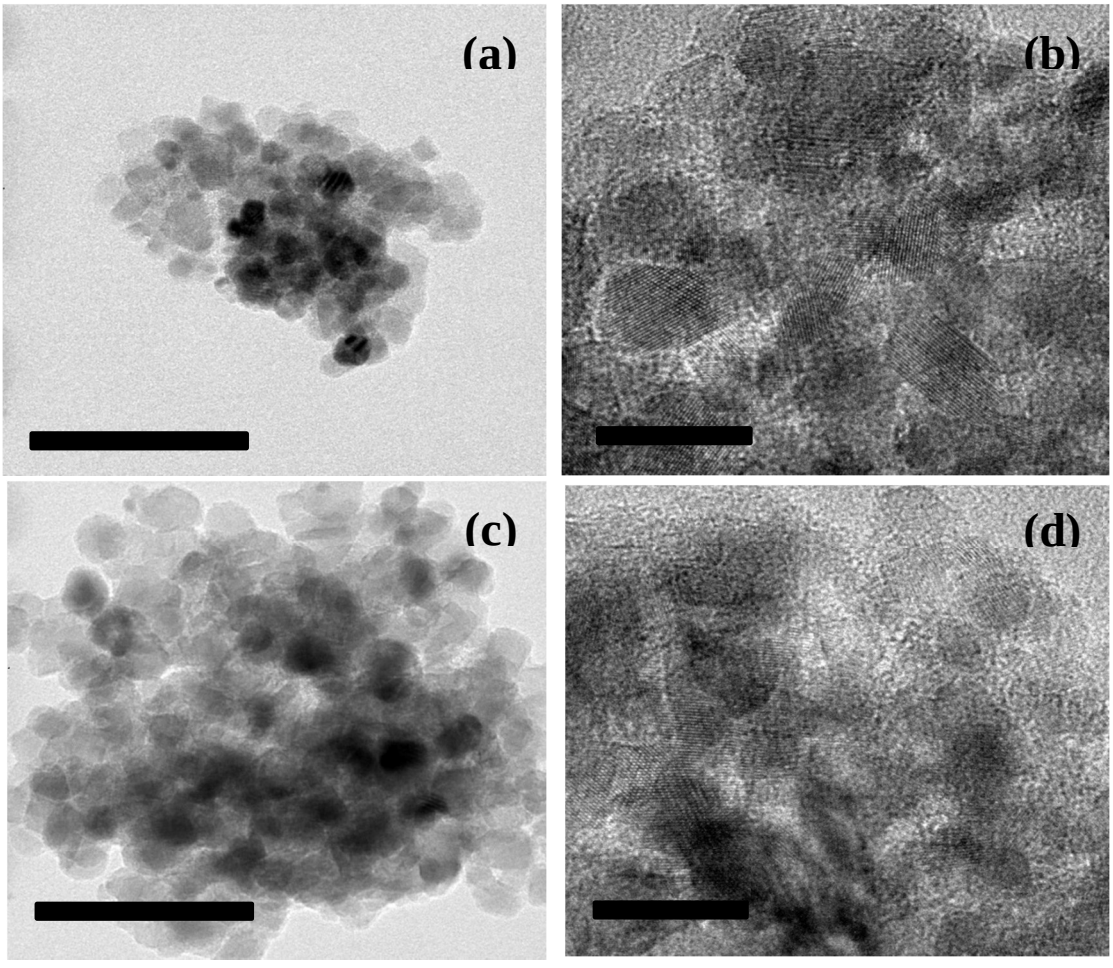

Fig.2. TEM images of (a) & (b) V-N co-doped TiO_2 and (c) & (d) un-doped TiO_2.

The optical absorption of the nitrogen, vanadium co-doped TiO_2 compounds were determined by diffuse reflectance spectroscopy (Fig. 3). The properties were calculated using the absorbance versus wavelength data based on Kubelka-Munk function, as shown in Fig. 3 (b). The co-doped samples show higher absorption in the visible light compared to pristine TiO_2. The band gap of undoped TiO_2, N2-TiO_2, V2-TiO_2 and V2N1-TiO_2 and V2N2-TiO_2 co-doped TiO_2 was found to be 3.1 eV, 2.94 eV and 2.80 eV, 2.62 eV and 2.54 eV respectively as shown in Fig. 3(a). Nitrogen doping into TiO_2 aided a significant reduction in the band gap by 0.16 eV. Similarly, V and N co-doping into TiO_2 has resulted in reduction of band gap by 0.48 and 0.56 eV respectively.

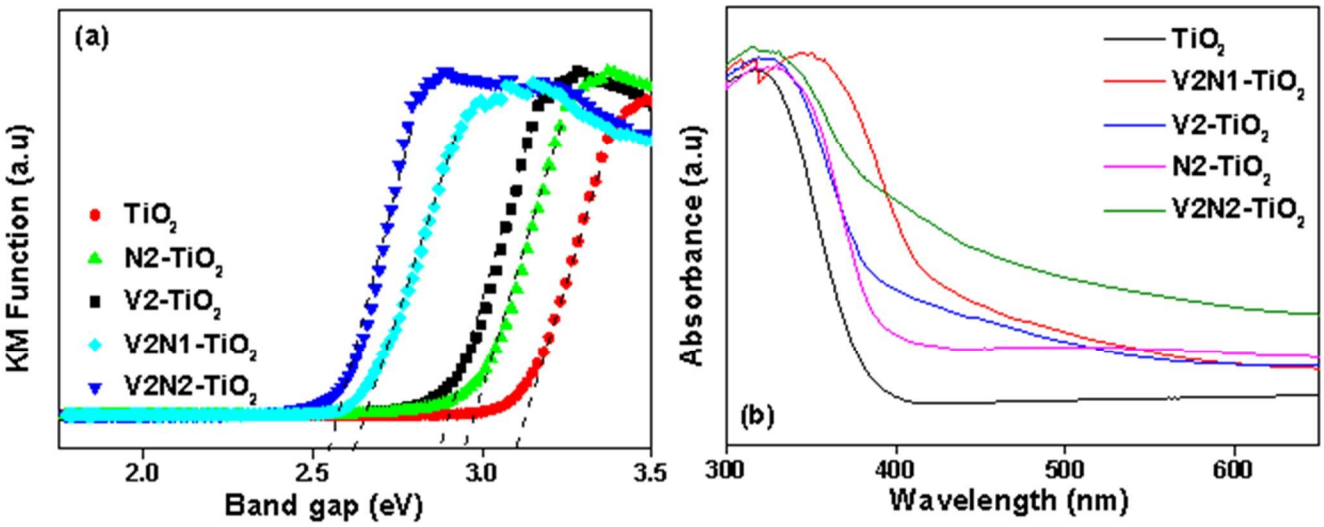

Fig.3. (a) KM plots and (b) Absorption spectra of TiO_2, N2-TiO_2, V2-TiO_2, V2N1-TiO_2 and V2N2-TiO_2 doped catalyst

This indicates that co-doping of nitrogen and vanadium results in creating additional energy levels between the conduction and valence band edge of TiO_2. This electronic transition from the dopant's electronic states to states of TiO_2 can effectively cause a red shift in band edge absorption threshold [25, 65]. The co-doping with nitrogen and vanadium induces the narrowing of the band gap of TiO_2. The metal ion implanted TiO_2 overlap the conduction band of d-orbital of TiO_2 [66].

It can be suggested that d-orbital overlapping from the dopant and parent lattice decreases the band gap of TiO_2 and enhances visible light absorption. 3d states of vanadium can occupy just below the conduction band of TiO_2 [67]. Vanadium existing in V 4+ and 3+ states, and electronic transition between these states can significantly enhance the absorption and narrowing the band gap. Further, it is well known that nitrogen doping can form new states that lie just above the valence band for the substituted nitrogen. However, for the interstitial nitrogen, the N-O bond generates localized states with p-orbitals [68]. This state lies below the O-2p band of TiO_2. This prevents additional states for the excited charge carriers and can prevent recombination. Therefore, nitrogen and vanadium doping resulted in the formation of new states close to the valence band and conduction band, respectively.

The chemical compositions and states of the elements in the TiO_2 ("Ti" in undoped TiO_2 and V2N1 co-doped TiO_2), and nitrogen ("N" in V2N1 and V2N2 co-doped TiO_2), vanadium ("V" in V2N1-TiO_2) co-doped TiO_2 were investigated by XPS analysis. The core level spectra of N-1s, Ti-2p and V-2p peaks are shown in Fig.4. The broad N-1s peak from 394 eV to 400 eV can be deconvoluted into two peaks at 396 eV and 400 eV respectively. The peak around 396 eV represents the nitrogen ions in the substituted form because the binding energy is close to Ti-N bond [69]. The peaks at higher binding energy can be attributed to O-Ti-N linkage and Ti-N-O linkage. This peak arising due to N-O bonds can be inferred to nitrogen existing in interstitial sites of TiO_2. However, it is still debatable that whether substitutional or interstitial nitrogen doping enhances the photocatalytic activity[70].

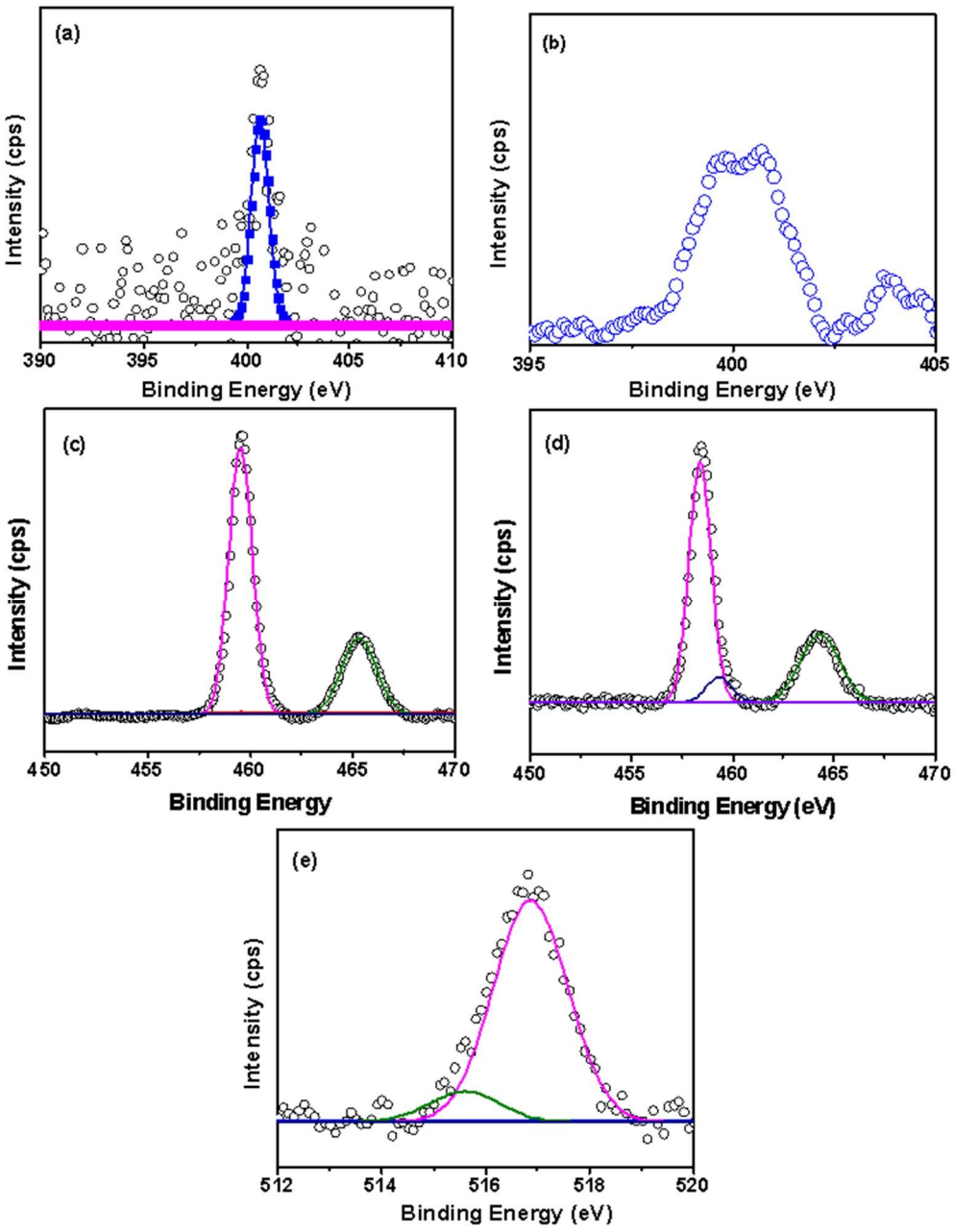

Fig.4. X-ray photoelectron spectroscopy plot for N-1s from (a) 1 atom % nitrogen doped V-TiO_2 (b) 2 atom % nitrogen doped V2-TiO_2, for Ti-2p from (c) un-doped TiO_2 and (d) V2N1 co-doped TiO_2 for V-2p from V2N1 co-doped TiO_2

Despite this, nitrogen doped TiO_2 has shown enhanced absorption in the visible light. N-1s peak of vanadium and nitrogen doped catalysts are represented in Fig.4 (a) and (b). Fig.4 (a) shows the N-1s peak in the interstitial state approximately around 401 eV. However, N-1s peak in Fig.4 (b) represents the presence of nitrogen in both substitutional and interstitial states. Usually, substituted nitrogen is observed around 396 eV. However, both substitutional and interstitial states are observed very close to each other. Few reports suggest that shifting of N-1s towards higher binding energy is possible because of reduction in electron density due to the presence of oxygen atoms [71]. Fig. 4 (c) and (d) represents the deconvolution of Ti-2p of Ti in undoped and doped catalysts. Fig. 4 (c) shows that Ti exists in 4+ state. Ti can be deconvoluted into $2p_{3/2}$ and $2p_{1/2}$. However, Ti in doped sample shows the presence of Ti in both 4+ and 3+ states indicating the presence of oxygen vacancies, as shown in Fig. 4 (d). Similarly, the presence of dopant in the TiO_2 lattice can be identified by the shift of Ti towards lower binding energy.

This decrease in binding energy is due to various interactions at electronic level of Ti-2p indicating the presence of vanadium and nitrogen in the lattice [72]. The deconvolution of V-2p as shown in Fig. 4 (e) peak suggests that vanadium exists in two different states such as V 5+ and 4+. Compared to their intensities, it can be suggested that the surface of doped TiO_2 consists of vanadium in 5+ state. The presence of vanadium in the TiO_2 lattice helps in the incorporation of nitrogen into the lattice. The lattice distortion created by vanadium ions facilitates reducing the resistance for nitrogen doping developed due to charge neutrality [73]. This was clearly observed from the amount of nitrogen doped into the TiO_2 lattice for the same precursor concentration. Nitrogen in N-doped TiO_2 was 0.24 atom % whereas in vanadium doped TiO_2 it was 0.62 atom % for the same concentration loading, suggesting incorporation of vanadium into TiO_2 lattice has reduced the barrier for nitrogen doping.

Photoluminescence of the co-doped samples supports the XPS spectra. The PL intensity of N-doped and V-N doped TiO_2 is lower compared to pristine TiO_2 as shown in Fig.5. This is evident from the fact that interstitial doped nitrogen acts as a trap for charge carrier species and it also aids in creation of oxygen vacancies which can be clearly noticed from XPS spectra of doped TiO_2. Similarly PL intensity of both V and N co-doped TiO_2 is significantly lower than pristine and N-doped TiO_2. It has been observed that the PL intensity of N2-TiO_2 is less than V2-TiO_2, similarly, both co-doped samples i.e, V2N1-TiO_2 and V2N2-TiO_2 has lower PL intensity than their individual counterparts. However, intensity of V2N1-TiO_2 is significantly lower than V2N2-TiO_2 indicating V2N1-TiO_2 prevents most of the recombination. This can also been observed from the photoactivity, where V2N1-TiO_2 degrades the pollutant faster than V2N2-TiO_2. The peaks at 420, 450, 490 and 530 nm can be observed in the PL spectra and they can be assigned to charge transitions from an oxygen vacancy trapped electron, recombination of self-trapped exciton and intrinsic states of TiO_2. Generally V-N co-doping aids in trapping the holes and also allows electron transfer between valence band and newly introduced defect states by V and N. The presence of available energy states in the form of vanadium and nitrogen ions has not only contributed in red shifting the band gap but also in the reduction of charge carrier recombination. Therefore, it is now clear that how N doped and V- N co-doped TiO_2 catalyst are more efficient than pristine TiO_2.

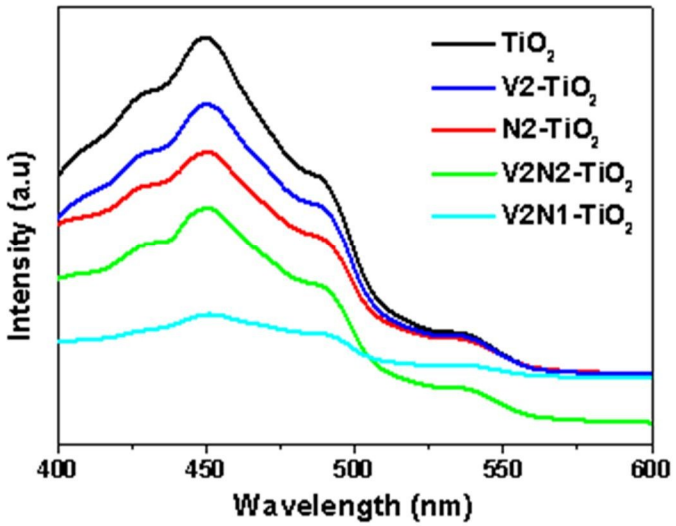

Fig.5. Photoluminescence spectra of TiO_2, N2-TiO_2, V2-TiO_2, V2N1-TiO_2 and V2N2-TiO_2 N doped catalyst

3.2. Photocatalysis

The photocatalytic activity of vanadium, nitrogen and vanadium-nitrogen co-doped TiO_2 samples for degrading antibiotic under visible light was determined and shown in Fig. 6. The degradation of antibiotic solution using pristine, N-doped, V-doped and V-N co-doped TiO_2 catalysts followed first order rate kinetics. The detailed results and kinetics are discussed below.

3.2.1. Effect of vanadium doping concentration: The V-doped TiO_2 samples were designated as V0.1, V0.2, V1 and V2, respectively, when the concentration of vanadium was varied between 0.1 – 2 atom %, as described above. The photocatalytic activity of V-doped TiO_2 increases gradually as the concentration of vanadium increases in the TiO_2 lattice till it reaches 2 atom % as shown in Fig. 6 (b). It can be suggested that the increase in concentration of vanadium not only decreases the band gap of the catalyst but also serves as charge trapping centers. This can be clearly seen that un-doped TiO_2 does not show much photocatalytic activity under visible light. Further increase in

concentration of vanadium decrease the photoactivity where the presence of more vanadium ions in the lattice might act as charge recombination centers for the photogenerated electron and holes. The variation of concentration with time for different concentrations of vanadium doped titania is shown in Fig. 6 (b). The degradation follows first order kinetics, as shown in Fig. 6 (e), and the rate constants are listed in Table 2.

3.2.2. Effect of nitrogen doping concentration: Nitrogen doped TiO_2 catalysts were prepared with triethylamine as nitrogen precursor. The N-doped catalysts were denoted according to their loading concentration such as N0.5, N1, N2 and N4, respectively. The photocatalytic activity of N-doped catalysts for degrading the antibiotic has increased gradually with respect to increase in nitrogen concentration until the concentration reached 2 atom %. Among all N-doped catalysts, N2 has shown better photocatalytic activity by degrading the antibiotic solution completely in 120 min as shown in Fig. 6 (a). As described, N-doped catalysts have performed better compared to un-doped TiO_2 under visible light, indicating nitrogen doping has enhanced visible light absorption. Further, the presence of 2p states N-1s enhances efficient charge transfer preventing recombination. The variation of concentration with time for different concentrations of nitrogen doped titania is shown in Fig. 6 (a). The degradation follows first order kinetics, as shown in Fig. 6 (d) and the rate constants are listed in Table 2.

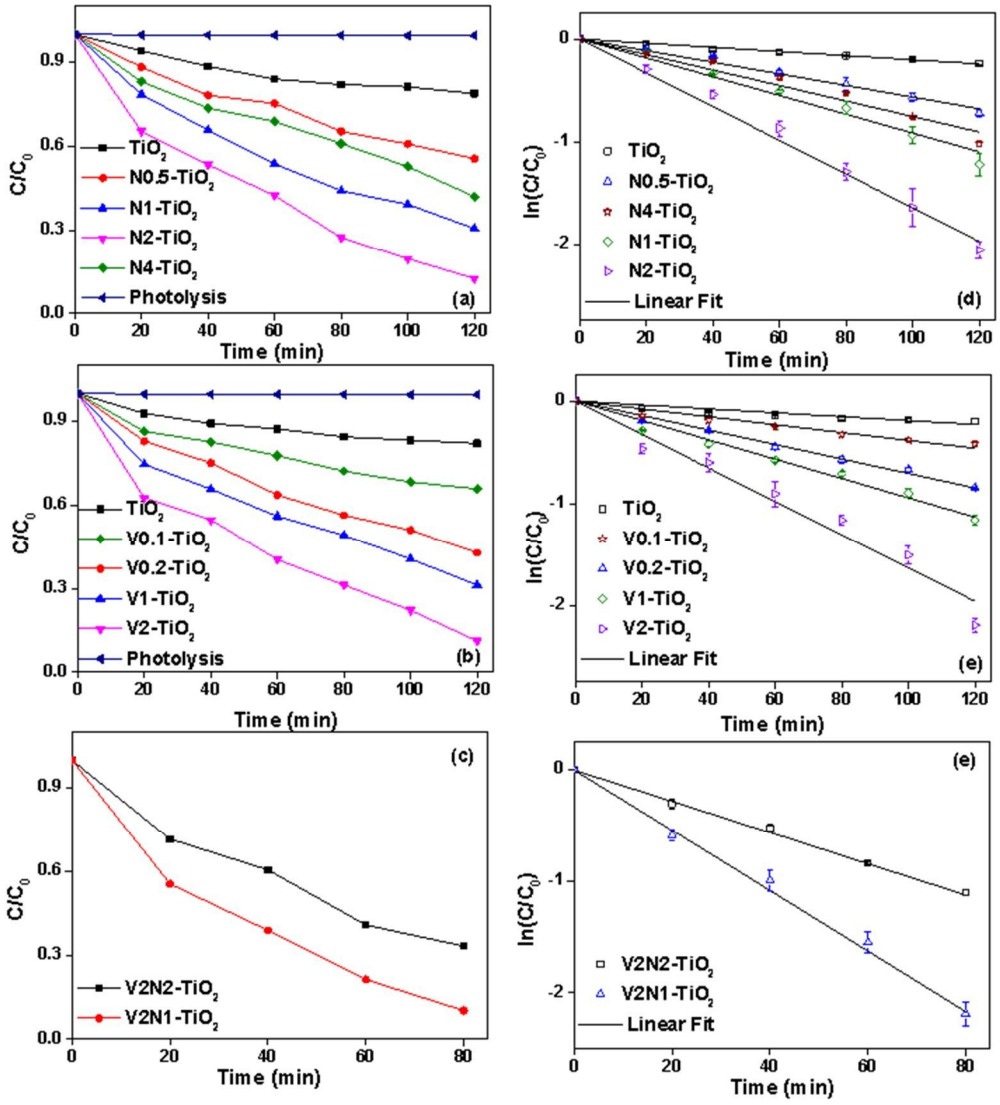

Fig.6. Photocatalytic degradation of antibiotic showing (a) effect of N-doping concentration (b) effect of V-doping concentration and (c) effect of V2N2 and V2N1 doping into TiO_2. Kinetics of photocatalytic degradation of antibiotic showing (d) effect of N-doping concentration (e) effect of V-doping concentration and (f) V2N2 and V2N1 doping into TiO_2.

Effect of vanadium doping concentration	
	Rate Constant ($k_{app} \times 10^{-4}$ min^{-1})
Catalyst	
TiO_2	20 ± 2
V0.1	38 ± 2
V0.2	71 ± 5
V1	95 ± 7
V2	165 ± 4

Effect of nitrogen doping concentration	
	Rate Constant ($k_{app} \times 10^{-4}$ min^{-1})
Catalyst	
TiO_2	20 ± 2
N0.5	56 ± 2
N1	92 ± 5
N2	164 ± 9
N4	75 ± 4

Effect of nitrogen doping concentration in vanadium doped TiO_2	
	Rate constant ($k_{app} \times 10^{-4}$ min^{-1})
Catalyst	
V2N1	325 ± 9
V2N2	195 ± 7

Table 2: Rate parameters of the photodegradation of chloramphenicol in the presence of various catalysts.

3.2.3. Effect of nitrogen concentration in V-N co-doped TiO_2: Vanadium and nitrogen co-doped TiO_2 catalysts were denoted as V2N1 and V2N2 respectively, where concentration of vanadium was maintained as constant (2 atom %) whereas for nitrogen it was varied from 1 – 2 atom %. This approach was followed for two reasons: as described above, photocatalytic activity of V-doped catalysts was higher if the concentration of vanadium was maintained as 2 atom %. The second reason is that it is known that nitrogen dopant in TiO_2 can be either substitutional or interstitial [74]. Therefore, the effect of a low and high concentration of nitrogen doping into vanadium distorted TiO_2 lattice was studied. The photocatalytic activity of V2N1 was significantly higher than V2N2 catalyst. The nitrogen in V2N1 catalyst was found to be in purely interstitial, whereas it is both interstitial and substitutional as that of in V2N2. The photocatalytic effect was better if a very low concentration of nitrogen was maintained. The variation of concentration with time for this case is shown in Fig. 6 (c). The degradation follows first order kinetics, as shown in Fig. 6 (e) and the rate constants are listed in Table 2.

Therefore, 2 atom % doping of vanadium into TiO_2 has significantly improved the photocatalytic activity. However, recombination of charge carriers is also higher, as shown in photoluminescence study. Similarly, increasing nitrogen content upto 4 atom % was also not favoring the high catalytic activity. Considering the XRD patterns into account, addition of either cationic or anionic dopants has not modified the crystal structure, as only anatase phase existed and no other impure phases were found. Band engineering should have got enhanced by co-doping vanadium and nitrogen into the TiO_2 lattice. However, restricting the quantity of nitrogen to 1 atom % enabled interstitial placement as observed from XPS studies, which enhanced the photoactivity under visible light efficiently by both reducing the band gap and preventing recombination effectively. Doping same quantity (1 atom % of nitrogen) alone in TiO_2 lattice has not provided

significant photoactivity. However, the activity enhanced tremendously in the presence of V ion inside TiO_2 lattice which suggests that strain developed by placement of vanadium ion has enabled more nitrogen influx into the lattice. Slight increment to 2 atom % of nitrogen into V-TiO_2 has led the nitrogen to be in substitutional state. From the experiments conducted, substitutional nitrogen in vanadium doped TiO_2 has much lower photocatalytic activity compared to interstitial nitrogen in V-TiO_2. This suggests that presence of foreign (cationic) ion and its quantity can modify the fate of nitrogen placement and in turn influence the photocatalytic activity. This paves the way towards necessity of potential assessment on metal and non-metal combined metal oxide studies based on their placement on TiO_2 lattice. However, except nitrogen, none of the other non-metals has been reported to occupy specific sites like nitrogen, providing a huge scope for further studies.

3.2.4. Effect of catalyst loading: The effect of catalyst amount in degrading the antibiotic solution was determined by varying the catalyst concentration as 0.5, 1, 2 and 3 g/l respectively. The rate of antibiotic degradation increased significantly as the loading increased till the loading concentration was 2 g/l (Fig. 7). The antibiotic degradation took long time when the concentration was 0.5 g/l and this is due insufficient amount of catalyst. The photocatalytic activity decreased for 3 g/l loading. This might due to insufficient photon availability for the catalyst particles and aggregation of the particles. The latter lead to reduction of the active surface area of catalyst and a subsequent decrease in photocatalytic activity.

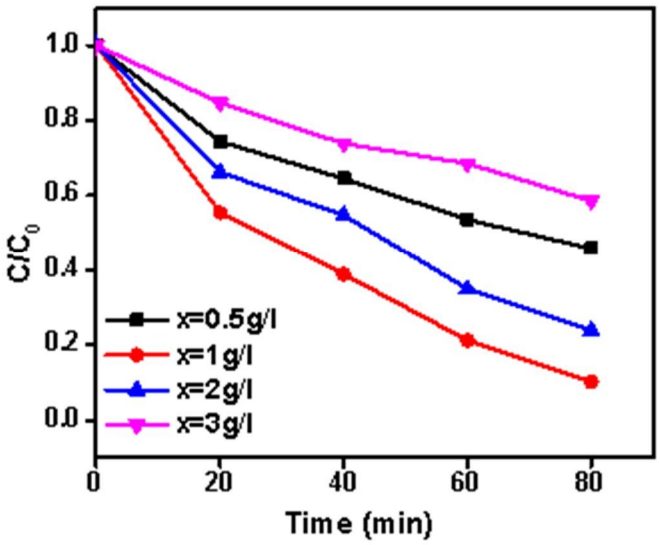

Fig.7. Photocatalytic degradation of antibiotic using V2N1 co-doped TiO_2 showing effect of catalyst loading (x = quantity of catalyst)

3.2.5. Effect of V-N doped TiO_2 catalyst against E.coli degradation under visible light: In addition to antibiotic degradation, the V-N co-doped TiO_2 catalysts were employed to determine its effect on killing micro-organisms under visible light, as shown in Fig. 8. The initial concentration of bacteria was maintained as 2×10^9 CFU/ml. During dark reactions, there was no significant decrease in bacterial concentration. The bacterial degradation was also determined due to the effect of light alone. Significant reduction was observed until 60 min and saturation was observed at higher time because of lack of decrease of bacterial concentration as shown in Fig. 8 (a). The catalysts were denoted as V0N0 and V2N1 for un-doped and doped TiO_2 catalysts. Bacterial degradation due to photolysis was noted from the decrease in bacterial colony forming units from 2.1×10^9 CFU/ml to 1.09×10^9 CFU/ml after 120 min. For the same time, cells concentration dropped from 2×10^9 CFU/ml to 2.9×10^5 CFU/ml for pristine TiO_2. Compared to undoped TiO_2, V-N co-doped TiO_2 has shown better photocatalytic microbial degradation, reducing number of bacteria from 2.1×10^9 CFU/ml to

1.04×10^{1} CFU/ml in just 120 min. The better antimicrobial activity of V-N co-doped TiO_2 catalyst might due to effective charge transport, better visible light absorption, decrease in charge recombination compared to undoped TiO_2. Effective charge carrier generation and separation produces hydroxyl radicals, which are responsible for anti-microbial activity by following cell membrane deterioration or inhibiting cellular functions by damaging DNA. This study has showed that V-N doped TiO_2 catalyst has significantly improved the antibacterial degradation in comparison to un-doped TiO_2 under visible light.

3.2.6. Effect of antibiotic and bacteria co-degradation using V-N co-doped TiO_2 under visible light: The novelty of this study is to determine the effect of co-degradation of both antibiotic and bacteria in their close vicinity simultaneously. This study was aimed to show that V-N co-doped catalyst can degrade the bacteria and excess of antibiotic in an ecosystem such that the bacterial resistance towards that specific antibiotic can be prevented. For this, bacterial suspension was taken in an antibiotic solution. The effect of antibiotic alone on the bacteria was also studied by suspending bacteria in the antibiotic solution without catalyst. The bacterial degradation in the presence of antibiotic, catalyst and antibiotic with catalyst was shown in Fig. 8 (b). It is known that chloramphenicol is bacteriostatic antibiotic. It prevents the bacteria from synthesizing proteins for various cellular functions by binding to their ribosomes thereby inactivating the bacteria [75]. There is no significant change observed in the bacterial concentration until 40 min. Later, reduction was observed. This might be due to the fact that effective passage of the antibiotic into the bacterial cells. Since the bacterial culture was tested initially for its anti-resistance against chloramphenicol, significant degradation of bacteria was observed when plated. For the co-degradation of antibiotic and bacteria in the presence of catalyst, 1 g/l of V-N co-doped catalyst was taken into bacterial-antibiotic suspension and kept under visible light for degradation.

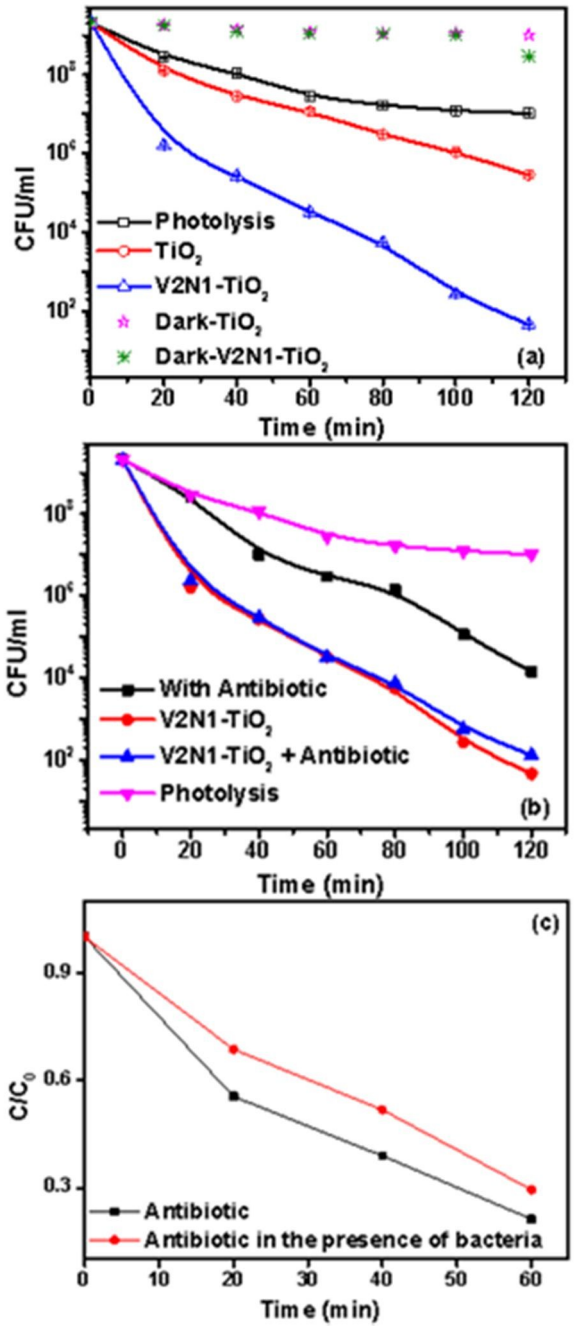

Fig.8. Photocatalytic anti-bacterial activity of (a) TiO_2 and V2N1-TiO_2 co-doped TiO_2 in dark and under visible light (b)V2N1-TiO_2 in the presence of antibiotic (c) showing antibiotic degradation in the presence and absence of bacteria

There is only a slight increase in degrading bacteria in the presence of antibiotic by the catalyst. However, the antibiotic degradation was observed simultaneously as shown in Fig. 8 (c). Though the rate of bacterial degradation in the presence of antibiotic has not changed significantly in the presence of catalyst alone, there is an effective in reduction of antibiotic concentration. The bacteria can allow the antibiotic to pass through their channels and hence there is decrease in concentration of antibiotic in the suspension [76]. Secondly, the photocatalyst will degrade the antibiotic present in the suspension. Here, bacteria that allow antibiotic to pass through their channels were also degraded simultaneously by the catalyst in addition to degradation of existing antibiotic outside the bacteria in the system. This will prevent the bacteria from developing resistance against the antibiotic and excess antibiotic in the stream also is degraded preventing possible microbial contact [77]. Hence, it was showed that V-N co-doped catalyst can degrade bacteria and antibiotic simultaneously under visible light that is of great importance in the current scenario of microbiological and pharmaceutical community.

3.2.7. Scavenger Experiments

Reactive oxygen radicals responsible for antibiotic degradation were analyzed by performing scavenger experiments. Reactive radical scavengers such as Ethylene diamine tetraacetic acid (EDTA), tertiary butyl alcohol (TBA), dimethyl sulphoxide (DMSO) and benzoquinone (BZQ) for the determination of the influence of hole, hydroxyl, superoxide and electron radicals, respectively. V2N1-TiO_2, which was found to be the best catalyst among all compositions investigated in this study, was taken in antibiotic suspension. 1 mM of each scavenger was added separately for each experiment to determine which reactive oxygen species is most responsible for the photodegradation. Among all scavengers, addition of EDTA decreased the photodegradation of antibiotic to ~80%, as shown Fig. 9. This indicates that holes are the major responsible reactive

radicals through which antibiotic degrade most. Similarly, addition of TBA, BZQ and DMSO reduced the degradation up to 74%, 55% and 30% respectively. Chloramphenicol itself contains positive charged amine species and electronegative chlorine. Therefore, attacking them by reactive oxygen species might significantly compromise its configuration and hence lose its antibiotic activity. Once the antibiotic starts degrading, its property to inhibit the bacteria will be restricted and subsequently, prolonged exposure towards bacteria can also be avoided.

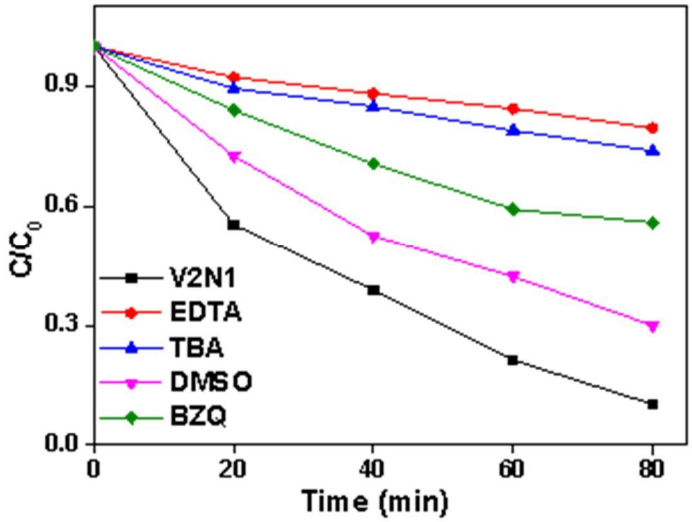

Fig.9. Scavenger experiments to identify responsible reactive oxygen species for the photodegradation of antibiotic by V2N1-TiO_2. (EDTA-Ethylene diamine tetraacetic acid, TBA-Tertiary butyl alcohol, DMSO-Dimethyl sulfoxide, BZQ-Benzoquinone).

3.2.8. Reusability: The reusability of the catalysts was studied by using the catalyst for repeated degradation of the antibiotic solution. As discussed above, both 1 g/l and 2 g/l loading of the catalyst has shown better photocatalytic activity against antibiotic degradation. Therefore, their reusability effect was determined by using the same catalyst for more than two consecutive degradation cycles, as shown in Fig. 10. After every cycle, the catalysts were washed with distilled water twice and heated at 100°C for 60 min and used further for the next cycle. Good photocatalytic activity was observed in the first cycle. However, the photoactivity of 2 g/l loading decreased gradually over subsequent cycles. This might be due to increase in aggregation of catalyst resulting in the reduction of the effective active surface area of the catalyst after every cycle. 1 g/l loading has shown consistent photocatalytic activity suggesting better reusability factor for this catalyst loading.

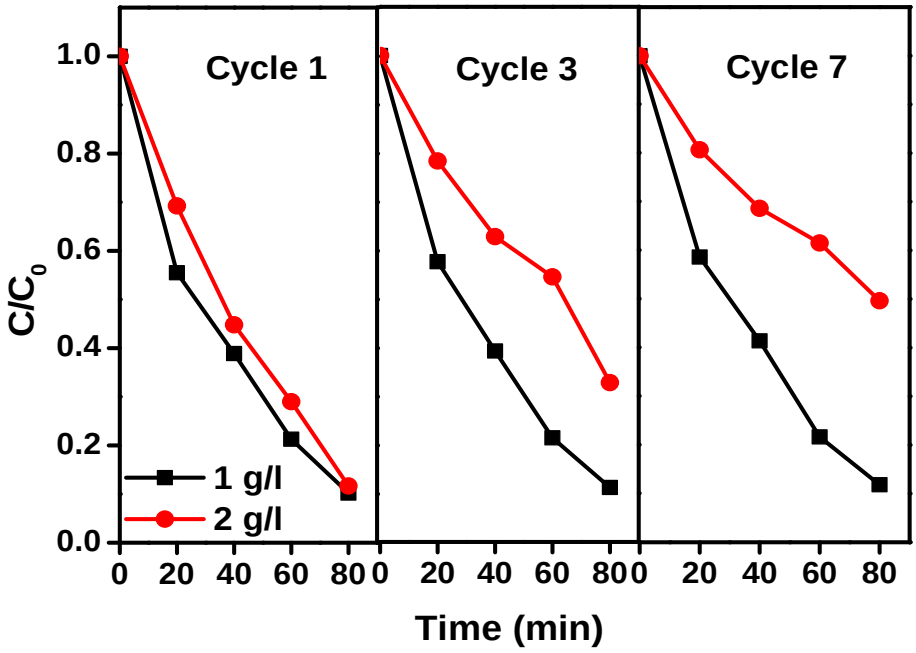

Fig.10. Reusability of V2N1-TiO_2 for photocatalytic activity.

To summarize, vanadium doping in TiO_2 could have possibly created trapping centers and charge migration on the semiconductor. This prevents recombination and decreases the band gap by forming localized V-2p states in TiO_2 band structure. Similarly, vanadium doping prior to nitrogen doping has efficiently increased the nitrogen dopant concentration by reducing the barrier for the non-metal dopant into TiO_2 lattice. Besides enhancing visible light absorption nitrogen doping also creates oxygen vacancies that facilitates efficient charge transport in the semiconductor. This enhances the lifetime of photogenerated holes and electrons during photocatalysis. Among two different states of nitrogen doping, this study clearly shows that interstitial nitrogen doping is more effective than substitutional doping for photocatalysis.

4. Conclusions

Vanadium and nitrogen co-doped TiO_2 catalysts were synthesized successfully for antibiotic and microbial degradation. The antibacterial activity of V-N co-doped TiO2 catalyst against E.coli was studied successfully. The photocatalytic activity was higher if the concentration of vanadium and nitrogen was maintained as 2 atom % and 1 atom %, respectively, in V-N co-doped catalysts. The effects of interstitial and substitutional nitrogen doping in V-doped TiO_2 catalysts were studied and it was shown that the photocatalytic antibiotic degradation was better under interstitial N-doping in V-doped TiO_2 catalyst. V and N doping has extended the absorption wavelength towards visible region and resulted in extending excellent charge transfer capability for higher photoactivity. Simultaneous antibiotic and bacterial degradation was successfully studied using V-N doped TiO_2. It was shown that this catalyst can efficiently degrade both the antibiotic and bacteria simultaneously preventing the bacteria from having prolonged contact with the antibiotic. Therefore, V-N doped TiO_2 was determined as a better photocatalyst to degrade both antibiotic and bacteria in their close vicinity under visible light.

Acknowledgements

The authors are thankful to the Department of Science and Technology for the financial assistance. The authors thank Prof. Jayant Modak for extending his facilities for bacterial work, Ms. Archana for assisting in DRS measurement and CeNSE, AFMM for characterization facilities.

References

1. B. Ohtani, *Physical chemistry chemical physics*, 2014, **16**, 1788-1797.
2. X. Chen and A. Selloni, *Chemical reviews*, 2014, **114**, 9281-9282.
3. L.-B. Mo, Y. Bai, Q.-Y. Xiang, Q. Li, J.-O. Wang, K. Ibrahim and J.-L. Cao, *Appl. Phys. Lett.*, 2014, **105**, 202114.
4. C. Dette, M. A. Perez-Osorio, C. S. Kley, P. Punke, C. E. Patrick, P. Jacobson, F. Giustino, S. J. Jung and K. Kern, *Nano Lett.*, 2014, **14**, 6533-6538.
5. N. Serpone, *J. Phys. Chem. B*, 2006, **110**, 24287-24293.
6. R. Asahi, T. Morikawa, T. Ohwaki, K. Aoki and Y. Taga, *Science*, 2001, **293**, 269-271.
7. K. Kobayakawa, Y. Murakami and Y. Sato, *J. Photochem. Photobiol. A: Chem.*, 2005, **170**, 177-179.
8. C. S. Enache, J. Schoonman and R. van de Krol, *Appl. Surf. Sci.*, 2006, **252**, 6342-6347.
9. J.-Y. Lee, J. Park and J.-H. Cho, *Appl. Phys. Lett.*, 2005, **87**, 1904.
10. J. C. Yu, J. Yu, W. Ho, Z. Jiang and L. Zhang, *Chem. Mater.*, 2002, **14**, 3808-3816.
11. D. Li, H. Haneda, S. Hishita, N. Ohashi and N. K. Labhsetwar, *J. Fluorine Chem.*, 2005, **126**, 69-77.
12. L. Lin, W. Lin, Y. Zhu, B. Zhao and Y. Xie, *Chem. Lett.*, 2005, **34**, 284-285.
13. S. Dong, J. Feng, M. Fan, Y. Pi, L. Hu, M. Liu, J. Sun and J. Sun, *RSC Advances*, 2015, **5**, 14610-14630.
14. Y. Zhu, Y. Wang, Z. Chen, L. Qin, L. Yang, L. Zhu, P. Tang, T. Gao, Y. Huang and Z. Sha, *Applied Catalysis A: General*, 2015, **498**, 159-166.
15. Z. Zhao, Y. Wang, J. Xu, C. Shang and Y. Wang, *Appl. Surf. Sci.*, 2015.
16. N. K. Eswar, P. Ramamurthy and G. Madras, *Photochemical & Photobiological Sciences*, 2015.
17. B. Liu, H. M. Chen, C. Liu, S. C. Andrews, C. Hahn and P. Yang, *J. Am. Chem. Soc.*, 2013, **135**, 9995-9998.
18. M. n. García-Mota, A. Vojvodic, F. Abild-Pedersen and J. K. Nørskov, *J. Phys. Chem. C*, 2012, **117**, 460-465.
19. Y. Wang, R. Zhang, J. Li, L. Li and S. Lin, *Nanoscale research letters*, 2014, **9**, 1-8.
20. K. Nagaveni, M. Hegde and G. Madras, *J. Phys. Chem. B*, 2004, **108**, 20204-20212.
21. A. Zaleska, *Recent Patents on Engineering*, 2008, **2**, 157-164.
22. C. Sotelo-Vazquez, N. Noor, A. Kafizas, R. Quesada-Cabrera, D. O. Scanlon, A. Taylor, J. R. Durrant and I. P. Parkin, *Chemistry of Materials*, 2015.
23. L. G. Devi and R. Kavitha, *Applied Catalysis B: Environmental*, 2013, **140**, 559-587.
24. C. Di Valentin and G. Pacchioni, *Catal. Today*, 2013, **206**, 12-18.
25. X. Chen and C. Burda, *Journal of the American Chemical Society*, 2008, **130**, 5018-5019.
26. T. Lindgren, J. M. Mwabora, E. Avendaño, J. Jonsson, A. Hoel, C.-G. Granqvist and S.-E. Lindquist, *J. Phys. Chem. B*, 2003, **107**, 5709-5716.
27. O. Diwald, T. L. Thompson, T. Zubkov, E. G. Goralski, S. D. Walck and J. T. Yates, *J. Phys. Chem. B*, 2004, **108**, 6004-6008.
28. Y. Cong, J. Zhang, F. Chen and M. Anpo, *The Journal of Physical Chemistry C*, 2007, **111**, 6976-6982.
29. C. Burda, Y. Lou, X. Chen, A. C. Samia, J. Stout and J. L. Gole, *Nano letters*, 2003, **3**, 1049-1051.
30. M. Sathish, B. Viswanathan, R. Viswanath and C. S. Gopinath, *Chemistry of Materials*, 2005, **17**, 6349-6353.
31. J. Varley, A. Janotti and C. Van de Walle, *Adv. Mater.*, 2011, **23**, 2343-2347.
32. L. Zeng, W. Song, M. Li, X. Jie, D. Zeng and C. Xie, *Appl. Catal. A: Gen.*, 2014, **488**, 239-247.
33. M. Ceotto, L. Lo Presti, G. Cappelletti, D. Meroni, F. Spadavecchia, R. Zecca, M. Leoni, P. Scardi, C. L. Bianchi and S. Ardizzone, *J. Phys. Chem. C*, 2012, **116**, 1764-1771.
34. J. Zhang, Y. Wu, M. Xing, S. A. K. Leghari and S. Sajjad, *Energy & Environmental Science*, 2010, **3**, 715-726.
35. C. Liu, X. Tang, C. Mo and Z. Qiang, *J. Solid State Chem.*, 2008, **181**, 913-919.

36. Z.-h. Yuan and J.-h. Jia, *Mater. Chem. Phys.*, 2002, **73**, 323-326.
37. Q. Zhang, T. Gao, J. M. Andino and Y. Li, *Appl. Catal. B: Environ*, 2012, **123**, 257-264.
38. J. Liu, R. Han, Y. Zhao, H. Wang, W. Lu, T. Yu and Y. Zhang, *The Journal of Physical Chemistry C*, 2011, **115**, 4507-4515.
39. D.-E. Gu, B.-C. Yang and Y.-D. Hu, *Catal. Commun.*, 2008, **9**, 1472-1476.
40. R. Jaiswal, N. Patel, D. Kothari and A. Miotello, *Appl. Catal. B: Environ*, 2012, **126**, 47-54.
41. S. Bagwasi, B. Tian, J. Zhang and M. Nasir, *Chem. Eng. J.*, 2013, **217**, 108-118.
42. S. Bagwasi, Y. Niu, M. Nasir, B. Tian and J. Zhang, *Appl. Surf. Sci.*, 2013, **264**, 139-147.
43. M. Nasir, S. Bagwasi, Y. Jiao, F. Chen, B. Tian and J. Zhang, *Chem. Eng. J.*, 2014, **236**, 388-397.
44. H. Hao and J. Zhang, *Microporous Mesoporous Mater.*, 2009, **121**, 52-57.
45. Y. Cong, J. Zhang, F. Chen, M. Anpo and D. He, *J. Phys. Chem. C*, 2007, **111**, 10618-10623.
46. Y. Niu, M. Xing, J. Zhang and B. Tian, *Catal. Today*, 2013, **201**, 159-166.
47. Y. Cong, B. Tian and J. Zhang, *Appl. Catal. B: Environ*, 2011, **101**, 376-381.
48. H. Liu, Y. Wu and J. Zhang, *ACS applied materials & interfaces*, 2011, **3**, 1757-1764.
49. Y. Ma, M. Xing, J. Zhang, B. Tian and F. Chen, *Microporous Mesoporous Mater.*, 2012, **156**, 145-152.
50. S. Klosek and D. Raftery, *J. Phys. Chem. B*, 2001, **105**, 2815-2819.
51. G. Carré, E. Hamon, S. Ennahar, M. Estner, M.-C. Lett, P. Horvatovich, J.-P. Gies, V. Keller, N. Keller and P. Andre, *Appl. Environ. Microbiol.*, 2014, **80**, 2573-2581.
52. C. Rodriguez, A. Di Cara, F. Renaud, J. Freney, N. Horvais, R. Borel, E. Puzenat and C. Guillard, *Catal. Today*, 2014, **230**, 41-46.
53. C. T. T. Binh, T. Tong, J. F. Gaillard, K. A. Gray and J. J. Kelly, *Environ. Toxicol. Chem.*, 2014, **33**, 317-327.
54. S. Adhikari, A. Banerjee, N. K. Eswar, D. Sarkar and G. Madras, *RSC Advances*, 2015, **5**, 51067-51077.
55. V. Lorian, *Antibiotics in laboratory medicine*, Lippincott Williams & Wilkins, 2005.
56. M. A. Kohanski, D. J. Dwyer and J. J. Collins, *Nature Reviews Microbiology*, 2010, **8**, 423-435.
57. K. Kümmerer, *J. Antimicrob. Chemother.*, 2003, **52**, 5-7.
58. E. Zuccato, D. Calamari, M. Natangelo and R. Fanelli, *The lancet*, 2000, **355**, 1789-1790.
59. C. A. Arias and B. E. Murray, *New Engl. J. Med.*, 2009, **360**, 439-443.
60. D. Ferber, *Science*, 2000, **288**, 792.
61. A. P. Magiorakos, A. Srinivasan, R. Carey, Y. Carmeli, M. Falagas, C. Giske, S. Harbarth, J. Hindler, G. Kahlmeter and B. Olsson-Liljequist*, Clinical Microbiology and Infection*, 2012, **18**, 268-281.
62. J. L. Martinez, *Environ. Pollut.*, 2009, **157**, 2893-2902.
63. A. K. Rumaiz, J. Woicik, E. Cockayne, H. Lin, G. H. Jaffari and S. Shah, *Appl. Phys. Lett.*, 2009, **95**, 262111.
64. X. Yang, C. Cao, L. Erickson, K. Hohn, R. Maghirang and K. Klabunde, *Applied Catalysis B: Environmental*, 2009, **91**, 657-662.
65. C. Di Valentin, E. Finazzi, G. Pacchioni, A. Selloni, S. Livraghi, M. C. Paganini and E. Giamello, *Chemical Physics*, 2007, **339**, 44-56.
66. S. T. Martin, C. L. Morrison and M. R. Hoffmann, *The Journal of Physical Chemistry*, 1994, **98**, 13695-13704.
67. J. C.-S. Wu and C.-H. Chen, *J. Photochem. Photobiol. A: Chem.*, 2004, **163**, 509-515.
68. C. Di Valentin, G. Pacchioni, A. Selloni, S. Livraghi and E. Giamello, *J. Phys. Chem. B*, 2005, **109**, 11414-11419.
69. M. Batzill, E. H. Morales and U. Diebold, *Phys. Rev. Lett.*, 2006, **96**, 026103.
70. C. W. Dunnill and I. P. Parkin, *Dalton Trans.*, 2011, **40**, 1635-1640.
71. H. Liu, G. Liu and X. Shi, *Colloids Surf. Physicochem. Eng. Aspects*, 2010, **363**, 35-40.
72. Y. Huang, W. Ho, Z. Ai, X. Song, L. Zhang and S. Lee, *Applied Catalysis B: Environmental*, 2009, **89**, 398-405.

73. Y. Nakano, T. Morikawa, T. Ohwaki and Y. Taga, *Appl. Phys. Lett.*, 2005, **87**, 232104.
74. H. Irie, Y. Watanabe and K. Hashimoto, *J. Phys. Chem. B*, 2003, **107**, 5483-5486.
75. G. Pankey and L. Sabath, *Clin. Infect. Dis.*, 2004, **38**, 864-870.
76. M. A. Kohanski, D. J. Dwyer, B. Hayete, C. A. Lawrence and J. J. Collins, *Cell*, 2007, **130**, 797-810.
77. C. F. Amábile-Cuevas, M. Cárdenas-García and M. Ludgar, *American Scientist*, 1995, 320-329.

Novel synergistic photocatalytic degradation of antibiotics and bacteria using V-N doped TiO_2 under visible light: State of nitrogen in V-doped TiO_2

*Neerugatti KrishnaRao Eswar [1], Praveen C Ramamurthy [1, 2] and Giridhar Madras [3]**

[1]Centre for Nanoscience and Engineering, [2]Dept. of Materials Engineering,

[3]Dept. of Chemical Engineering, Indian Institute of Science, Bangalore-560012

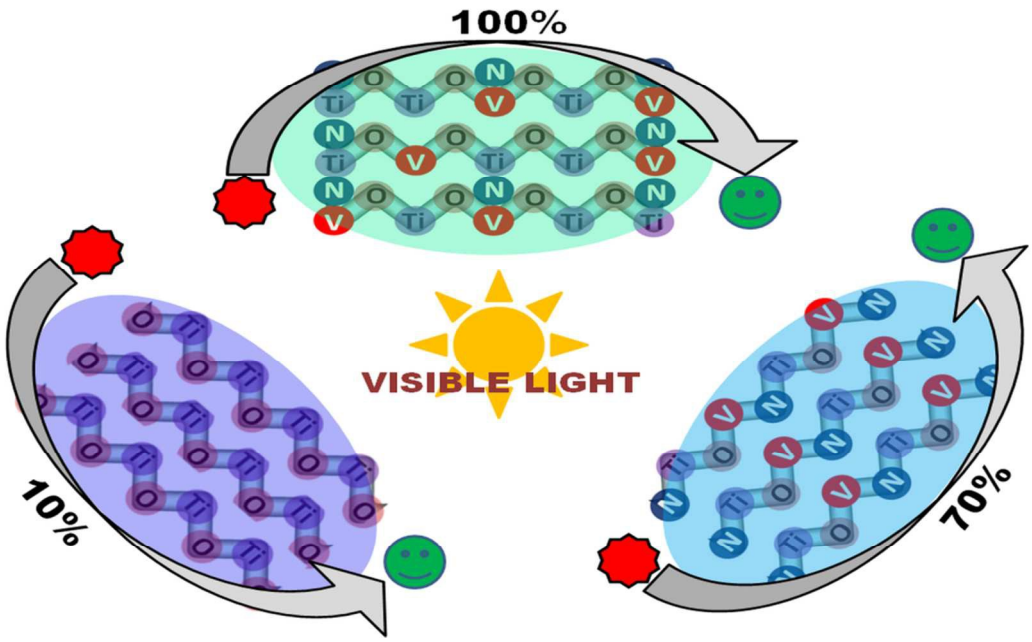

Interstitial and substitutional nitrogen co-doped in vanadium-TiO_2 for the simultaneous photocatalytic antibiotic degradation and bacterial inactivation